Desalination and Water Treatment
www.deswater.com

doi: 10.1080/19443994.2015.1136964

57 (2016) 23873–23892
October

Taylor & Francis
Taylor & Francis Group

Ammonium removal from landfill leachate using natural zeolite: kinetic, equilibrium, and thermodynamic studies

Fulya Aydın Temel[a,*], Ayşe Kuleyin[b]

[a]*Engineering Faculty, Department of Environmental Engineering, Giresun University, 28200 Giresun, Turkey, Tel. +90 454 3101740, ext. 4038; email: fulya.temel@giresun.edu.tr*
[b]*Engineering Faculty, Department of Environmental Engineering, Ondokuzmayıs University, 55139 Samsun, Turkey, Tel. +90 362 3121919, ext. 1319; email: akuleyin@omu.edu.tr*

Received 23 April 2015; Accepted 16 December 2015

ABSTRACT

The scope of this study is to research the removal of NH_4-N from landfill leachate using natural Turkish zeolite by adsorption process. The effects of pH (2–8), contact time (5–1,440 min), adsorbent dosage (30–150 g L^{-1}), agitation speed (100–300 rpm), initial concentration (263.2–1,363.6 mg L^{-1}), and particle size (10–65 mesh) were examined on the adsorption process. The optimum conditions in the adsorption process were established as follows: pH (its pH value of leachate), 60 min of contact time, 100 g L^{-1} of adsorbent dosage, 200 rpm of agitation speed, 263.2 mg L^{-1} of initial concentration, and −20 + 35 mesh of particle size. The adsorption kinetics and isotherms were tested to understand the adsorption mechanism using three kinetic models, i.e. Elovich, intraparticle diffusion, the pseudo-second-order reaction kinetic models, and four isotherm models, i.e. Dubinin–Radushkevich, Langmuir, Tempkin, and Freundlich isotherm models. Correlation coefficients, kinetic, and isotherm parameters were calculated. It was shown that the best conformity kinetic model was the pseudo-second-order reaction kinetic model ($R^2 > 0.99$) for the present study. According to the results obtained from isotherms experiments, the adsorption equilibrium was defined well by the Langmuir and Tempkin isotherm model for NH_4-N adsorption onto zeolite. The thermodynamic parameters were also detected. The values of Gibbs free energy (ΔG°), enthalpy (ΔH°), and entropy of activation (ΔS°) were 5.7113–6.5018 kJ mol^{-1}, −8.5415, and 8.8209 J mol^{-1} K^{-1}, respectively. They were showed that the NH_4-N adsorption process onto zeolite was an exothermic physical adsorption process, randomness, and non spontaneous in the temperature range studied (25–60°C). Results indicate that zeolite is the most efficient cation exchanger for NH_4-N removal from landfill leachate.

Keywords: Leachate; NH_4-N; Zeolite; Kinetic; Isotherm; Thermodynamic

1. Introduction

Sanitary landfilling is the most widely method used for management of municipal solid waste (MSW) among the different alternatives due to its economic advantages [1]. Solid waste composition shows variety based on location, season/climate, and socioeconomic developments of region, waste collection, and disposal methods of the municipal corporation. Solid wastes substantially consist of organic substances. Most of the

*Corresponding author.

organic substances have biologically degradable property. They can degrade simpler compounds by micro-organisms by changing according to the environmental conditions. Thus, the leachate and gas occur in the sanitary landfilling region [2]. The composition of landfill leachate changes depending upon the solid waste composition, the conditions of the landfill such as temperature, pH, moisture content, age, and geometry of landfill, the properties of the water entering in the landfill, and the type of soil adjacent to the landfill [3].

Leachate containing various hazardous pollutants is produced in large quantities by landfills. These pollutants can be divided into four main groups: (i) inorganic compounds, such as NH_4-N, Ca, Mg, Na, K, Fe, SO_4, and Cl, (ii) dissolved organic matter, (iii) heavy metals, such as Ni, Cu, Cd, Pb, Cr, and Zn, and (iv) xenobiotik organic materials [4]. Among these pollutants, ammonium is found high concentrations. There are several conventional removal technologies by the way of ex-situ treatment. Biological nitrification–denitrification, chemical precipitation, air-stripping, adsorption, ion exchange, breakpoint chlorination, and reserve osmosis are mainly among the NH_4-N removal technologies [5,6].

One of the most frequently used technologies in wastewater treatment is adsorption with activated carbon. However, the researchers have investigated the applicability of adsorption using cheaper raw materials due to the high cost of activated carbon. Recently, various materials have been used as an influential and alternative adsorbent to activated carbon for pollutants removal from contaminated water such as natural zeolite [7–9], pumice [10], illite [11], hazelnut shells [12], vermiculite [13,14], montmorillonite [15,16], volcanic tuff [17], clarified sludge [18], banana pith [19], sludge ash [20], sawdust [21–23], waste of tea [24], chitosan [25,26], clay [27], and others.

One of the distinctive properties of zeolites among porous materials is variety of pore shapes and sizes. Other properties of zeolites such as ion exchange and intercrystalline pores that are made different strong acidic sites, different molecules dimension, and active reservoirs for metal-catalyzed reactions have provided themselves widespread industrial uses. Zeolites that have large empty spaces or cages within their structures are among the most important inorganic cation exchangers. The structure of zeolites can accommodate large cations such as Na^+, K^+, Br^+, Mg^{2+}, and Ca^{2+}, and cationic groups such as H_2O, NH_4^+, CO_3^{2-}, and NO_3^-. Zeolites have properties such as good resistance to temperature, ionizing radiations, high cation exchange selectivity, and perfect compatibility with the environment. Therefore, zeolites as an alternative and influential adsorbent are located in modern technology [28].

The objective of present study is to research the adsorption capacity of Gördes zeolite for the NH_4-N removal from landfill leachate. Not evaluated of Gördes zeolite which exists excess quantity is an economic loss. Therefore, Gördes zeolite was investigated whether it was an alternative adsorbent or not. The influence of experimental conditions (pH, adsorbent dosage, contact time, particle size, agitation speed, and initial concentration) was examined and optimum conditions were evaluated for these experimental parameters. Kinetic (Elovich, intraparticle diffusion and pseudo-second-order reaction kinetic model) and equilibrium (Langmuir, Freundlich, Tempkin, and Dubinin–Radushkevich) models were used to further understand mechanism of adsorption process on zeolite. Thermodynamic parameters such as the standard free energy (ΔG°), entropy change (ΔS°), and enthalpy change (ΔH°) were also carried out to decide the suitability of NH_4-N adsorption on zeolite. And regenation of Gördes zeolite was investigated to check reusability of adsorbent.

2. Materials and methods

2.1. Adsorbent

The zeolite materials used in present study were provided from Rota Mining located in the city of Manisa in Turkey. Rota Mining has the world's highest quality zeolite reserves with 95% purity. Rota Mining is Turkey's largest manufacturer and marketer of natural zeolite minerals and one of the world's five largest natural zeolite mineral producers. Gördes zeolite was researched whether an alternative adsorbent or not in this study due to produce large quantities. Gördes zeolite has the following characteristics: purity of 92%, density of 2.15 g mL^{-1}, pore diameter of 4 Å, apparent density of 1.30 g mL^{-1}, bed porosity of 40%, a cation-exchange capacity of 1.9–2.2 meq g^{-1}, and suspension pH of 7.5–7.8. The chemical analysis of Gördes zeolite ground to –63 microns was conducted by inductively coupled plasma (ICP) (Perkin Elmer Model 3800). The surface area of this particular zeolite is 11.80 m^2 g^{-1} [29]. Thermal resistance is lower than 700°C [30,31]. SEM micrograph of Manisa–Gördes zeolite is given Fig. 1. The zeolitized tuffs have drusy texture with very high microporosity. XRD spectrum of natural zeolite is shown in Fig. 2. The chemical characteristics of zeolite are given in Table 1. When considered mineralogical content of zeolite, it is composed of mainly clinoptilolite (85%), feldspar (10%), and clay (5%) [32,33].

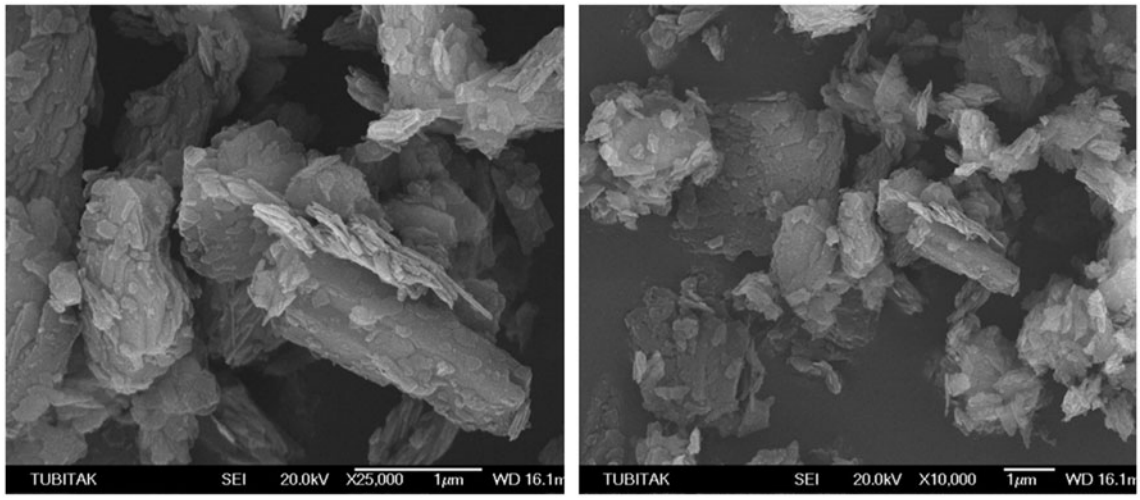

Fig. 1. SEM micrograph of natural Manisa–Gördes zeolite.

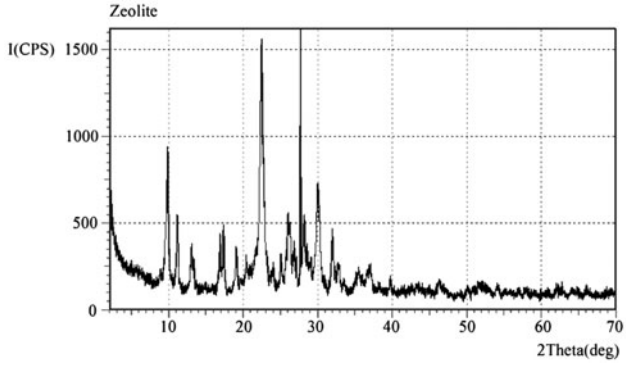

Fig. 2. XRD spectrum of natural Manisa–Gördes zeolite.

Table 1
EDXRF results of Gordes (Manisa) zeolite

Oxide	% Conc.	Elements	% Conc.
Na_2O	0.817	Al	6.769
MgO	0.232	K	2.719
Al_2O_3	12.789	O	50.432
SiO_2	80.736	Si	37.739
K_2O	3.275	Na	0.606
CaO	0.927	Mg	0.140
Fe_2O_3	0.699	Ca	0.663

The zeolite samples were milled, sifted and classified into four different size groups: –10 + 20 mesh size, –20 + 35 mesh size, –35 + 45 mesh size, and –45 + 65 mesh size. Then, they were washed with distilled water to clean fine particles and were dried at 35–60°C to remove moisture. The preconditioning was made to understand its effect on the removal efficiencies. The preconditioning studies were performed with 1-N NaCl and 2-N NaCl solutions at the temperature of 70°C and 200 rpm for 24 h to increase the remove efficiency of NH_4-N from landfill leachate using classified natural zeolite.

2.2. Adsorbate

The wastewater used in this study was procured from Yılanlı Dere Landfill located in the city of Samsun in Turkey. Yılanlı Dere Landfill was operated by Samsun Municipality between 1983 and 2008. About 400 ton/day solid waste were stored in this landfill. Leachate samples were provided from landfill basin and were stored at 4°C for experiments. The samples were analyzed according to the standard methods [34]. Table 2 summarizes the main characteristics of leachates used in this study.

2.3. Kinetic and equilibrium experiments

Kinetic experiments were conducted to detect influence of contact time on the NH_4-N adsorption capacity of the zeolite. In the experiments, four different particle sizes of zeolite and their preconditioning forms were tested. Zeolite sample of 5.0 g was mixed with leachate of 50 mL desired concentration with adsorbent/adsorbat ratio of 0.1 g mL^{-1} for 5–1,440 min in an orbital stirrer at room temperature and 200 rpm. Two phases of mixture obtained from different erlenmayer flasks were separated by filtration at interval time. The supernatant was analyzed as per method laid down in standard methods [34].

Table 2
Leachate characterization of Yılanlıdere landfill site

Parameters	Min. value (mg L^{-1})	Max. value (mg L^{-1})	Average value (mg L^{-1})
pH	6.5	8.62	7.95
COD	5,000	16,000	11,000
NH_4-N	1,078	1,596	1,247
BOD_5	3,000	10,000	6,400
Phosphates	9.8	42	23.37
Sulfates	872	2,013	2,279
Nitrates	9.5	32	21.1
Zn	0.11	0.28	0.21
Ni	0.16	0.21	0.19
Mn	0.11	0.43	0.27
Cr	0.08	0.16	0.12
Pb	0.07	0.2	0.14
Cu	0.03	0.09	0.06
Fe	0.6	2.45	1.44
Conductivity (ms cm^{-1})	16.5	19.47	18.56

Adsorption isotherm models for NH_4-N removal were also investigated. Equilibrium experiments were conducted to detect influences of four different particle sizes, three different agitation speeds, and temperatures on NH_4-N adsorption using eight different initial concentrations with an adsorbent dosage of 0.1 g L^{-1}, contact time of 1 h, its pH value of leachate. The selected zeolite form according to the results obtained from the kinetic experiments was used in all equilibrium experiments. The initial and final NH_4-N concentrations in the supernatant were analyzed. Quantities of NH_4-N adsorbed by samples were detected from the reduction of NH_4-N in the leachate. All kinetic and equilibrium experiments were performed in conical flasks of 250 mL with 50 mL wastewater.

The amount of NH_4-N adsorbed per gram adsorbent is detected as:

$$q_t = \frac{(C_o - C_t)V}{M} \quad (1)$$

and the following relationship is used to calculate the removal efficiency of adsorbate by the adsorbent:

$$\text{Adsorption}\,(\%) = \frac{(C_o - C_t)}{C_o} \times 100 \quad (2)$$

where q_t is quantity of the adsorbate exchanged per unit weight of the adsorbent at t time (mg g^{-1}), V is volume of the solution (L), M is mass of the adsorbent added to the solution (g), C_o and C_t are the adsorbate concentrations of initial and t time in the solution (mg L^{-1}), respectively.

3. Results and discussions

3.1. Effect of pH

The pH value of solution influences the surface charge of adsorbents like the degree of ionization of different pollutants. The adsorption process through dissociation of functional groups on the adsorbent surface active sites is affected by change of pH in the liquid because the hydrogen and hydroxyl ions are adsorbed quite strongly [35]. The optimum pH value of each pollutant in the adsorption process changes depending on changing pH value.

In this study, the influence of pH on NH_4-N adsorption by Turkish zeolite was investigated to detect the optimum value of pH. The experiments were performed using various pH values of leachate in range of 2–8 with an adsorbent dosage of 100 g L^{-1} using treated with 2-N NaCl of −20 + 35 mesh at temperature of 25°C and agitation speed of 200 rpm for 60 min. The pH values of landfill leachate were adjusted with H_2SO_4 or NaOH solutions.

Fig. 3 shows the influence of pH on removal of different initial NH_4-N concentrations. As is seen from Fig. 3, the adsorption capacity of NH_4-N at equilibrium was not significantly changed with the increasing pH in all cases. The pH has little influence on NH_4-N removal in range of 6–8 and the highest value was determined as 67.66% at pH 7. These results are agreement with the data of previous studies [32,36,37]. When the pH value is above 8 and below 6, NH_4-N removal was decreased slightly. At higher pH values, NH_4-N is neutralized by hydroxyl. At lower pH values than 6, NH_4-N removal is decreased due to competition of H^+ and NH_4^+ ions for the exchange

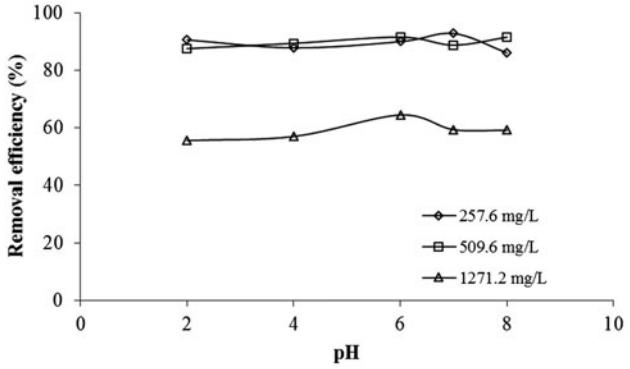

Fig. 3. Influence of pH on the NH_4-N removal by zeolite.

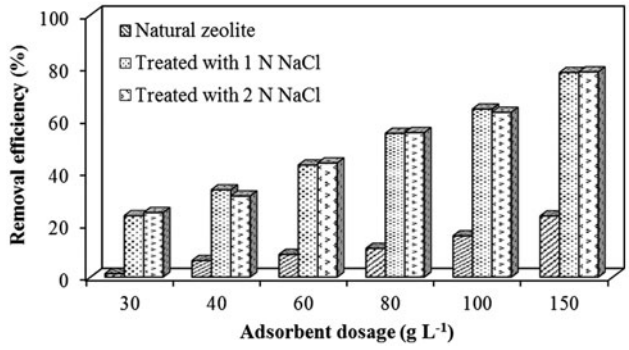

Fig. 4. The comparation of the effects of adsorbent dosage on the adsorption of NH_4-N.

sites in the zeolite surfaces [38]. According to the results obtained from the experiments for all initial concentrations, the influence of pH on the removal efficiency of NH_4-N was not observed to be significant. Hence, all further experiments were performed without pH adjustment.

3.2. Effect of adsorbent dosage

In order to research the effect of adsorbent dosage on removal efficiency of NH_4-N, the experiments were conducted with a wide dosage range of −20 + 35 mesh from 30 to 150 g L^{-1}, and the constant initial NH_4-N concentration at the agitation speed of 200 rpm and the temperature of 25°C without pH adjustment for 60 min. The preconditioning process with 1-N and 2-N NaCl solutions was applied the zeolite samples sieved the particle size of −20 + 35 mesh to saturate the exchange sites with sodium ions. Then zeolite samples (natural, treated with 1-N NaCl solution, and treated with 2-N NaCl solution) were used to detect the optimum conditions for NH_4-N removal in these experiments. The comparison of the effects of the adsorbent dosage on NH_4-N removal is given in Fig. 4.

As it is seen from Fig. 4, the removal of NH_4-N increased with increasing both modify of zeolites and adsorbent dosage. NH_4-N removal efficiencies of treated zeolite with 2-N NaCl were changed from 25 to 78% at increasing adsorbent dosages of 30–150 g L^{-1}. The adsorption of NH_4-N was not varied significantly between 100 and 150 g L^{-1} adsorbent dosage. Hence, the optimum adsorbent dosage of modified zeolite with 2-N NaCl solution was selected as 100 g L^{-1} for subsequent experiments.

3.3. Effect of contact time

These experiments are important to detect the required time for the adsorption equilibrium time. The influence of contact time ranging between 5 and 1,440 min on the adsorption of NH_4-N were performed at the temperature of 25°C, agitation speed of 200 rpm, initial concentration of 1,386 mg L^{-1}, and optimum adsorbent dosage of −20 + 35 mesh with natural zeolite, zeolite samples treated with 1-N NaCl and 2-N NaCl solutions without pH adjustment and corresponding graph is given in Fig. 5.

The adsorption of NH_4-N by Turkish zeolite increased rapidly with increasing contact time in the first 30 min for all cases and thereafter increased slowly till equilibrium time. According to the results, equilibrium times were reached in 12 h for natural zeolite, 4 h to treat with 1-N NaCl solution, and 1 h for treated with 2-N NaCl solution. After those times, no more NH_4-N was adsorbed. The removal efficiencies of NH_4-N at the equilibrium times were observed as 48% for natural zeolite, 60% for zeolite treated with 1-N NaCl solution, and 64% for zeolite treated with 2-N NaCl solution. It means that the removal of NH_4-N by zeolite treated with 2-N NaCl solution was observed better than the others. In all further

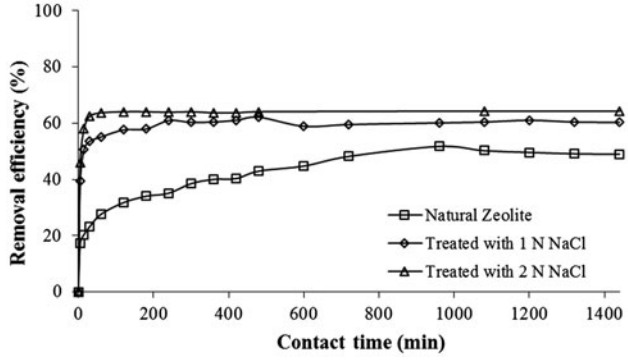

Fig. 5. The influence of contact time on the adsorption of NH_4-N.

experiments, the equilibrium time of 1 h was taken as the optimal contact time.

3.4. Effect of particle size with contact time

The other significant parameter in the adsorption process is particle size of the adsorbent. The adsorption capacity is based on the specific or external surface of the adsorbent [39]. The experiments were conducted in the four different particle sizes ranging between 10 and 65 mesh (−10 + 20, −20 + 35, −35 + 45, and −45 + 65 mesh) as a function of contact time at the temperature of 25˚C, agitation speed of 200 rpm, and optimum adsorbent dosage of 100 g L^{-1} without pH adjustment. The influent of particle size on the removal of NH_4-N from landfill leachate onto Turkish zeolite is shown in Fig. 6. As it is seen from Fig. 6, the adsorption capacity of zeolite decreased slightly with the increasing of particle size. It is clearly seen that the particle size of the adsorbent was very significant factor for adsorption capacity. The amount of NH_4-N adsorbed were determined as 7.84 mg g^{-1} for −10 + 20 mesh, 8.68 mg g^{-1} for −20 + 35 mesh, 7.784 mg g^{-1} for −35 + 45 mesh, and 7.868 mg g^{-1} for −45 + 65 mesh at the equilibrium contact time of 60 min. After that time, the variations of adsorption capacities were not significant. According to the results obtained from the experiments, the optimal adsorption capacity was provided with the particle size of −20 + 35 mesh. For this reason, −20 + 35 mesh was used in the subsequent experiments.

3.5. Effect of agitation speed with contact time

The adsorption capacity is controlled by film or/and intraparticle diffusion. Film diffusion is usually significant at the initial stages of the adsorption process. The ion mobilitiy increases in the solution when the favorable agitation speed is applied the adsorbent–adsorbate mixture and as a consequence of that the mass transfer resistance reduces [40–42]. In most cases, the increasing agitation speed results in an increase in the adsorption capacity, particularly during the initial periods of the process [40].

The effect of agitation speed ranging from 100 to 300 rpm by varying the contact time was investigated on the adsorption capacities of NH_4-N. The experiments were conducted at temperature of 25˚C, without pH adjustment, with an optimal adsorbent dosage of 100 g L^{-1} using zeolite treated with 2-N NaCl solution of −20 + 35 mesh during 1,440 min of contact time.

Fig. 7 gives the experimental results obtained from the effect of agitation speed with contact time. As it is shown in Fig. 7, the adsorption capacity of NH_4-N was not changed significantly with the increasement in agitation speed. The removal efficiencies and amount of NH_4-N adsorbed were determined as 61.60% and 8.176 mg g^{-1}, 64.06% and 8.68 mg g^{-1}, 63.75% and 8.568 mg g^{-1} at 100, 200, and 300 rpm, respectively. The agitation speed of 200 rpm seemed to be more appropriate in this study when the experimental results were evaluated.

3.6. Effect of initial concentration with contact time

The amount of NH_4-N adsorbed is a function of the initial adsorbate concentration. The adsorption capacities of NH_4-N were studied to evaluate at four different initial concentrations ranging from 263 to 1,363 mg L^{-1} by changing contact time in this section. The experiments were performed at agitation speed of 200 rpm, temperature of 25˚C, without pH adjustment, with the optimum adsorbent dosage of 100 g L^{-1} using

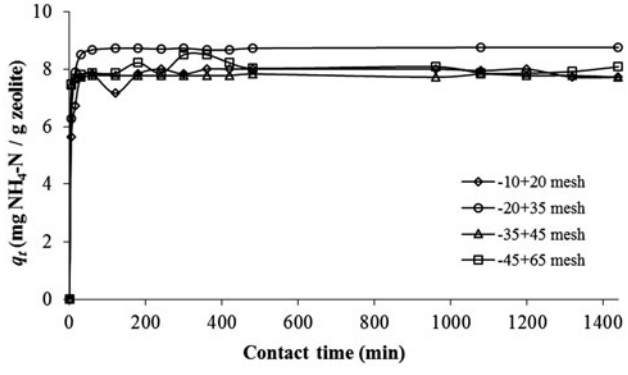

Fig. 6. The influence of particle size on the removal of NH_4-N.

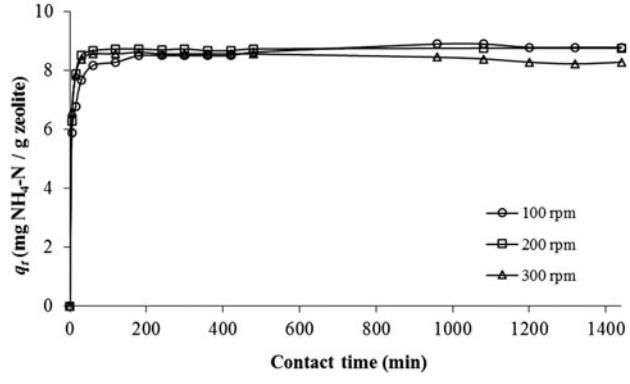

Fig. 7. Influent of agitation speed on the adsorption capacity of NH_4-N.

zeolite treated with 2-N NaCl solution of −20 + 35 mesh during 1,440 min of contact time.

The effects of initial NH_4-N concentrations onto Turkish zeolite are shown in Fig. 8. The adsorption capacity of the adsorbent increased with the increasing NH_4-N concentration whereas the removal efficiencies decreased with the increasing initial concentration as 92.55% for 263.2 mg L^{-1}, 87.5% for 515.2 mg L^{-1}, 78.57% for 940.5 mg L^{-1}, and 63.65% 1,363.6 mg L^{-1}, respectively. At lower initial concentrations, NH_4-N in the landfill leachate could contact with the binding sites on the adsorbent and thus the removal efficiencies of NH_4-N were better than the other cases. In contrast to this, the removal efficiencies of NH_4-N decreased because of the limited adsorption sites at higher initial concentrations. According to these results, it is recommended that before the wastewater is given in the adsorption units of wastewater treatment plant, the initial concentration of NH_4-N should reduce to increase the removal efficiency of NH_4-N and the life of the adsorbent.

3.7. Statistical analysis

To detect normality assumption validation we used Shapiro Wilks test statistic. According to the results of the test statistic $p = 0.000 < \alpha = 0.05$ we concluded that normality assumption was not valid for each group of agitation speeds, particle sizes, and initial concentrations. Because, there were more than two groups to compare (agitation speeds, particle sizes, and initial concentrations), we used Kruskall Wallis as a test statistic. According to the results of the test statistic $p = 0.029 < 0.05$ for agitation speeds, $p = 0.000 < 0.05$ for particle size and initial concentration, we concluded that at least one of the sources was different from others. To compare each source with other sources, we applied Mann Withney U test statistic. The results are given in Table 3. From table we could conclude that there was no difference between 200 and 300 rpm, there was no difference between (−10 + 20 mesh) and (−35 + 45 mesh), there was difference between all pairwise comparisons.

To detect normality assumption validation we used Shapiro Wilks test statistic. According to the results of the test statistic $p = 0.174 > \alpha = 0.05$ we concluded that normality assumption was valid for each group of initial concentrations in the effect of pH value. Because, there were more than two groups to compare, we used One-way ANOVA as a test statistic. According to the results of the test statistic $p = 0.000 < 0.05$, we concluded that at least one of the concentration was different from others. From the Levene's homogenity test of error variance we revealed that error variance was not homogen ($p = 0.024 < \alpha = 0.05$). In the case of inhomogeneity, we used Tamhane test to compare each concentration with other. The results are given in Table 3. According to the table we could conclude that there was difference between all pairwise comparisons.

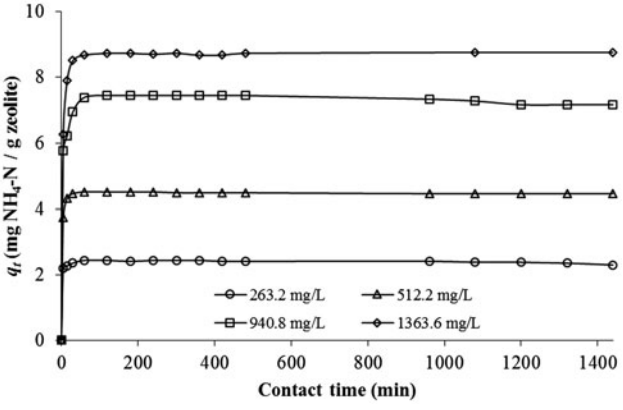

Fig. 8. Influent of initial concentration on the adsorption capacity of NH_4-N.

3.8 Adsorption kinetics

Different kinetic models were tested to get information about the behavior of the adsorbent under different experimental conditions (initial concentration of NH_4-N, agitation speed, and particle size of adsorbent). The conformity between the values estimated by model and experimental data are defined by coefficient of determination (R^2). A relatively high R^2 value remarks that the model describes successfully the kinetics of adsorption on adsorbent [33]. Different kinetic models namely Elovich, intraparticle diffusion, and pseudo-second-order reaction kinetic models were tested to research the adsorption of NH_4-N on zeolite.

3.8.1. Elovich model

The Elovich equation modified by Chien and Clayton was applied to research the kinetic of NH_4-N adsorption and desorption [33]. The Elovich equation is commonly used to detect the chemisorption on heterogeneous adsorbents, and is quite limited, as it only defines a limiting characteristic ultimately reached by the kinetic graph [43]. The Elovich equation is expressed as follows [44]:

$$\frac{dq_t}{dt} = \alpha \exp(-\beta q_t) \quad (3)$$

Table 3
Pairwise comparison results

	Source	*p*-value
pH	(257.6 mg L^{-1})–(509.6 mg L^{-1})	0.002[a]
	(257.6 mg L^{-1})–(1,271.2 mg L^{-1})	0.000[a]
	(509.6 mg L^{-1})–(1,271.2 mg L^{-1})	0.000[a]
Agitation speed	100–200 rpm	0.034[a]
	100–300 rpm	0.017[a]
	200–300 rpm	0.650
Particle size	(–45 + 65 mesh)–(–20 + 35 mesh)	0.000[a]
	(–45 + 65 mesh)–(–10 + 20 mesh)	0.035[a]
	(–45 + 65 mesh)–(–35 + 45 mesh)	0.000[a]
	(–20 + 35 mesh)–(–10 + 20 mesh)	0.002[a]
	(–20 + 35 mesh)–(–35 + 45 mesh)	0.000[a]
	(–10 + 20 mesh)–(–35 + 45 mesh)	0.160
Initial concentration	(263.2 mg L^{-1})–(515.2 mg L^{-1})	0.000[a]
	(263.2 mg L^{-1})–(940.8 mg L^{-1})	0.000[a]
	(263.2 mg L^{-1})–(1,363.6 mg L^{-1})	0.000[a]
	(515.2 mg L^{-1})–(940.8 mg L^{-1})	0.000[a]
	(515.2 mg L^{-1})–(1,363.6 mg L^{-1})	0.000[a]
	(940.8 mg L^{-1})–(1,363.6 mg L^{-1})	0.000[a]

[a]Statistically significant at 5%.

along with the boundary conditions it was assumed that $\alpha\,\beta > t$, the Elovich model equation is rewritten in its linear form as:

$$q_t = \frac{1}{\beta}\ln(\alpha\beta) + \frac{1}{\beta}\ln t \quad (4)$$

where q_t (mg g^{-1}) is the adsorption capacity of adsorbent at t time (min), α and β are the Elovich model parameters, α indicates the rate of chemisorption at zero coverage (mg g^{-1} min^{-1}), β is a constant corresponding to the surface coverage and activation energy for chemisorption (g mg^{-1}), and t is the contact time (min). The equation constants are calculated from the intercept and slope of straight line plot of q_t against ln t.

3.8.2. Intraparticle diffusion model

The intraparticle diffusion model recommended by Weber and Morris is expressed as [45,46]:

$$q_t = K_{id}\,t^{1/2} + C \quad (5)$$

where q_t (mg g^{-1}) is the adsorption capacity of adsorbent at t time (h), t is the contact time (h), K_{id} is the rate constant of intra-particle diffusion model (mg g^{-1} $h^{-1/2}$), C is a constant which gives an information to the boundary layer thickness (mg g^{-1}). K_{id} and C values are calculated from the slope and intercept of linear plot of q_t vs. $t^{1/2}$, respectively.

The adsorbate transfer to the adsorbent particles is identified by three stages as follows: film diffusion, intraparticle diffusion and adsorption. If the graph presents multi-linearity, the adsorption process is affected more than one step. The first stage is the diffusion of adsorbate from the liguid to the external surface of adsorbent namely film diffusion. The second stage defines the gradual adsorption step where intraparticle diffusion is rate limiting namely intraparticle diffussion. The third stage is expressed to the recent equilibrium step [47].

3.8.3. Pseudo-second-order reaction kinetic model

The pseudo-second-order kinetic model is tested to the adsorption of dyes, organic substances, and metal ions from wastewater [48]. The pseudo-second-order reaction kinetic depends on the assumption that chemisorption is dominant in the adsorption process [18,40,49,50]. The pseudo-second-order reaction kinetic model improved by Ho and McKay is defined as [7,51]:

$$\frac{dq_t}{dt} = k_2 (q_e - q_t)^2 \quad (6)$$

If the relationship is integrated for the boundary conditions $q_t = 0$ at $t = 0$ and $q_t = q_t$ at $t = t$, the linearized form of the relationship is achieved as:

$$\frac{t}{q_t} = \frac{1}{k_2 q_e^2} + \frac{t}{q_e} \quad (7)$$

The initial adsorption rate h (mg g^{-1} min^{-1}) is written by:

$$h = k_2 q_e^2 \quad (8)$$

where q_e and q_t (mg g^{-1}) are the adsorption capacities at equilibrium and desired time t (min), respectively. t is the contact time (min), k_2 is the velocity constant of model (g mg^{-1} min^{-1}). The model rate parameters k_2, q_e and h is obtained from slope and intercept of the plot of t/q_t vs. t.

Adsorption kinetic studies were performed to understand the behavior of zeolite for NH_4-N adsorption. The constants of kinetic models and correlation coefficients obtained from kinetic graphs for NH_4-N adsorption on zeolite were listed in Table 4. As is shown Table 4, the pseudo-second-order kinetic model for the all parameters showed the best fit. The model graphs for different experimental conditions (agitation speed, particle size, and initial concentration) are given in the Figs. 9, 10, and 11, respectively.

Good correlation coefficients as compared with the others were obtained for the pseudo-second-order reaction kinetic model with the correlation coefficients much higher than 0.99 (Table 4). However, its calculated equilibrium adsorption capacities (q_e) are found closer to the equilibrium adsorption capacities from experiments. It is indicated that chemisorption is the determining step of adsorption process rather than mass transfer from wastewater. The adsorption capacity (q_e) increased with increasing temperature which is typical chemisorption nature of adsorption. These facts indicate that the pseudo-second-order adsorption mechanism is predominant and explain the chemisorption of NH_4-N onto zeolite.

The graphs of Elovich model which is generally an application to chemisorption kinetics are given in Figs. S1–S3. The model regression coefficients were calculated from these graphs ($R^2 = 0.37$–0.87) and were showed in Table 4. Lower correlation coefficients detected from experimental results indicate that adsorption mechanism is not explained by the Elovich model.

Elovich and pseudo-second-order reaction kinetic models cannot express the diffusion mechanism. Therefore, the experimental data were applied the intraparticle diffusion model to understand the diffusion mechanism. The intraparticle diffusion model plots are presented in Figs. S4–S6 of supplementary part and experimental results obtained from the model are shown in Table 4.

The graphs suggest that the adsorption is composed of more than one step. The dual nature of the plots was procured due to the changeable extent of adsorption in the first and final stages of the experiments in all cases. This can be attributed to the fact that the adsorption in the final portion was the intraparticle diffusion while the adsorption in the first portion was the film diffusion. Table 4 also shows that the intercept (C) values increase with increasing agitation speed and decreasing particle size at 25˚C, but the straight lines did not pass through the origin ($C \neq 0$). The larger intercept means that it will be the contribution of the surface adsorption in the rate controlling step [46]. These deviations from origin in all cases indicate that the diffusion of NH_4-N in pores is not the only determining factor controlling the mechanism of the adsorption process. Therefore, both film diffusion and intraparticle diffusion processes in the adsorption of NH_4-N onto zeolite are significant. The adsorption mechanism is complex and external plus intraparticle diffusion contributes to the actual adsorption process.

In conclusion, the pseudo-second-order reaction kinetic model was observed to present better correlations of the experimental data. Thus, it suggests that the rate-limiting step can be chemisorption rather than diffusion.

3.9. Adsorption isotherm models

Adsorption isotherm models are important to define the relationships between molecules or ions in adsorbate and surface sites of adsorbent [52]. The one of necessary stages is to constitute the most favorable correlation for the equilibrium curves to optimize the design of an adsorption system [35]. There are several isotherm equations used for the equilibrium modeling of adsorption process. The experimental data obtained from NH_4-N adsorption onto zeolite were applied different adsorption isotherm models, namely, Langmuir, Freundlich, Tempkin, and Dubinin–Radushkevich adsorption isotherm models under different experimental conditions (agitation speed, particle size, and temperature) in this study.

Table 4
The constants and correlation coefficients of kinetic models for the removal of NH_4-N by zeolite

	Pseudo-second-order kinetic model				Elovich model			Intraparticle diffusion model					
	q_e	k_2	h	R^2	α	β	R^2	C_1	$K_{id,1}$	R_1^2	C_2	$K_{id,2}$	R_2^2
Agitation speed (rpm)													
100	8.8574	0.0160	1.2545	0.9998	1.55×10^5	2.1968	0.8669	4.6411	4.2819	1	8.1374	0.1566	0.8548
200	8.7719	0.0783	6.0241	1.000	4.56×10^8	3.0864	0.6019	4.8873	5.3606	0.9396	8.6807	0.0162	0.3559
300	8.2850	−0.0195	−1.3369	0.9998	1.59×10^{17}	5.618	0.3681	5.4784	4.2874	0.9576	8.7516	−0.0908	0.8105
Particle size (mesh)													
−10 + 20	7.8493	−0.0798	−4.914	0.9994	3.45×10^8	3.4423	0.603	4.2327	4.9514	0.9999	7.7352	0.0411	0.055
−20 + 35	8.7719	0.0783	6.0241	1.000	4.56×10^8	3.0864	0.6019	4.8873	5.3606	0.9396	8.6807	0.0162	0.3559
−35 + 45	7.7700	−0.2177	−13.1406	0.9999	2.47×10^{94}	29.1545	0.4266	7.3	0.6713	0.7551	7.7983	−0.0048	0.0392
−45 + 65 mesh	7.9618	−0.0321	−2.0338	0.9995	3.75×10^{36}	11.5075	0.2815	7.5275	0.2752	0.596	8.8036	−0.1878	0.6358
Initial concentration (mg L^{-1})													
515.2	4.4504	−0.1862	−3.6873	1.000	2.47×10^{24}	14.5349	0.4027	3.3364	1.676	0.8965	4.5293	−0.0173	0.9139
940.8	7.1891	−0.0254	−1.3134	0.9998	1.43×10^{12}	4.8852	0.5100	5.1045	2.3648	0.9751	7.6453	−0.0927	0.8587
1,363.6	8.7719	0.0783	6.0241	1.000	4.56×10^8	3.0864	0.6019	4.8873	5.3606	0.9396	8.6807	0.0162	0.3559

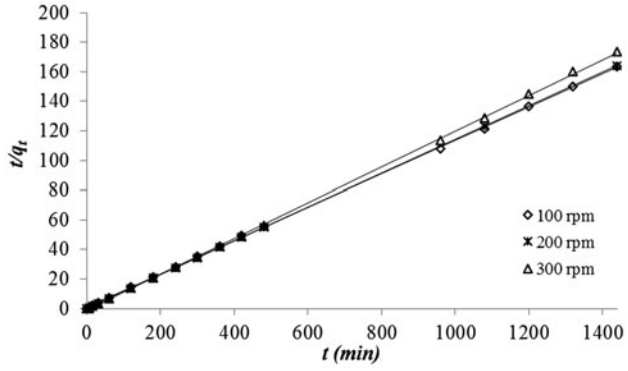

Fig. 9. Pseudo-second-order reaction kinetic models for agitation speeds.

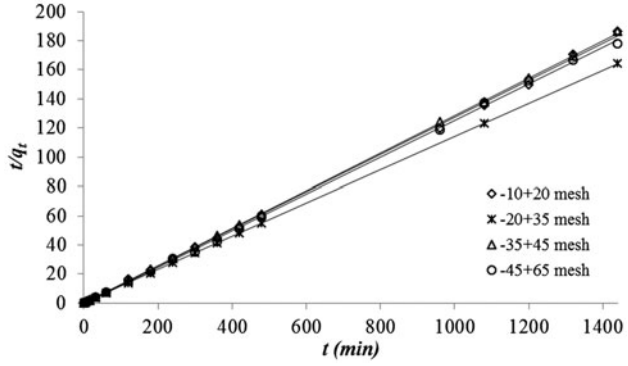

Fig. 10. Pseudo-second-order reaction kinetic models for particle sizes.

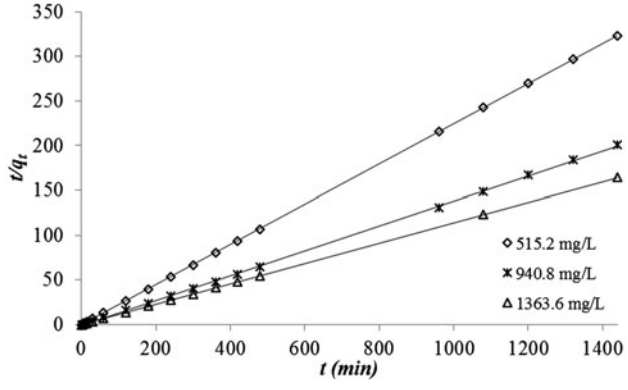

Fig. 11. Pseudo-second-order kinetic models for initial concentrations.

3.9.1. Langmuir isotherm

Three assumptions constitute the basic of the Langmuir isotherm model: the monolayer adsorption occurs onto adsorbent surface, each site of adsorbent hold homogeneity with adsorbate molecule and is energetically equivalent; adsorption in one site is not affected from the neighboring sites [46,52,53]. The nonlinear form of Langmuir isotherm model is written as [46,54]:

$$q_e = \frac{q_m K_L C_e}{1 + K_L C_e} \tag{9}$$

where C_e is concentration of NH_4-N (mg L^{-1}) at the equilibrium, q_e is the quantity of adsorbate adsorbed per unit mass of adsorbent at equilibrium (mg g^{-1}), q_m is the calculated maximum adsorption capacity (mg g^{-1}), and K_L is the energy constant related to the heat of adsorption or the adsorption intensity namely Langmuir adsorption constant (L mg^{-1}). The Langmuir constant K_L is a measure of the affinity between adsorbate and bindings sites of adsorbent.

Eq. (9) can be reformulated for the linear form of Langmuir isotherm model as:

$$\frac{C_e}{q_e} = \frac{1}{K_L q_m} + \frac{C_e}{q_m} \tag{10}$$

Both model constants (K_L and q_m) is obtained from intercept and slope from the plot of C_e/q_e against C_e.

The essential characteristics of Langmuir isotherm model is used to estimate relationships between adsorbate and adsorbent using a dimensionless equilibrium parameter or constant separation factor, R_L, defined by the following relationship:

$$R_L = \frac{1}{(1 + K_L C_0)} \tag{11}$$

where C_0 is the initial concentration of adsorbate (mg L^{-1}). The value of R_L gives information associated with the nature of adsorption. The value of R_L indicates the type of Langmuir isotherm to be irreversible ($R_L = 0$), favorable ($0 < R_L < 1$), linear ($R_L = 1$) or unfavorable ($R_L > 1$) [39,46,52].

3.9.2. Freundlich isotherm

The Freundlich model supposes that the adsorption process is occurred on a heterogeneous surface. The model provides knowledge with regard to the surface heterogeneity, and the exponential distribution of active sites and their energies [55]. The Freundlich model is generally given as follows [55,56]:

$$q_e = K_F C_e^{1/n} \tag{12}$$

The model equation is reformulated for the linear form by taking the ln of both sides as:

$$\ln q_e = \ln K_F + \frac{1}{n} \ln C_e \quad (13)$$

where q_e is the quantity of adsorbate adsorbed at equilibrium (mg g^{-1}), C_e is the equilibrium concentration of NH_4-N (mg L^{-1}), and K_F and n are Freundlich adsorption isotherm constants. K_F relates to the adsorption capacity of the adsorbent. The value of n relates to the adsorption intensity that varies with degree of heterogeneity. When the value of $1/n$ is $0 < 1/n < 1$, the adsorption is favorable; when $1/n = 1$, the adsorption is linear and irreversible; and when $1/n > 1$, the adsorption is a chemical process and unfavorable. The value of $1/n < 1$ means that adsorption capacity is only slightly suppressed at lower equilibrium concentrations and the adsorption process is a physical [46,52]. The values of K_F and n are detected by plotting ln q_e vs. ln C_e. The values of $1/n$ and K_F are equal to the slope and the intercept, respectively.

3.9.3. Tempkin isotherm

The Tempkin isotherm which considers the interactions between adsorbate and adsorbent supposes that: (i) the adsorption heat of all the molecules in the layer decreases linearly with coverage due to adsorbate-adsorbent interactions and (ii) adsorption is described by a uniform distribution of binding energies [35,57]. Tempkin isotherm model is explained as the following relationship [58]:

$$q_e = \frac{RT}{b(\ln A C_e)} \quad (14)$$

$$q_e = \frac{RT}{b}(\ln A) + \frac{RT}{b}(\ln C_e) \quad (15)$$

$$B = \frac{RT}{b} \quad (16)$$

where q_e is the quantity of adsorbate adsorbed at equilibrium (mg g^{-1}), C_e is the equilibrium concentration of NH_4-N (mg L^{-1}), B and b are the Tempkin constants associated with heat of adsorption (J mol^{-1}). A is the equilibrium binding constant in respect to the maximum binding energy (L g^{-1}), R is the gas constant (8.3145 J mol^{-1} K^{-1}), and T is the absolute temperature (K). The isotherm constants, A and B are calculated from intercept and slope from a plot of q_e vs. ln C_e, respectively.

3.9.4. Dubinin–Radushkevich (D–R) isotherm

The Dubinin–Radushkevich isotherm model is tested to evaluate the characteristic porosity, the apparent free of adsorption and the nature of the adsorption as chemical or physical [59,60]. The D–R adsorption isotherm is a more general model as its derivation is not based on ideal assumptions such as a constant adsorption potential or a homogeneous surface [60–62]. The empirical equation suggested by D–R has been widely applied to define the adsorption of gases and vapors on microporous solids [59]. The adsorption capacity per unit surface area of the adsorbent in the D–R isotherm model at equilibrium, q_e, is written as follows [63]:

$$q_e = q_m e^{-\beta\varepsilon^2} \quad (17)$$

The linear presentation of D–R isotherm equation is reformulated as:

$$\ln q_e = \ln q_m - \beta\varepsilon^2 \quad (18)$$

where q_e is the quantity of adsorbate adsorbed per unit mass of adsorbent (mg g^{-1}), q_m is the maximum adsorption capacity (mg g^{-1}), β is the activity coefficient associated with mean adsorption free energy (mol^2 kJ^{-2}). The constants β and q_m are detected from the slope and the intercept from the graph of ln q_e vs. ε^2, respectively.

$$\varepsilon = RT \ln\left(1 + \frac{1}{C_e}\right) \quad (19)$$

and ε is the Polanyi potential which is relation with the equilibrium concentration, R is the universal gas constant (8.3145 J mol^{-1} K^{-1}), T is the absolute temperature (K), and C_e is the concentration of adsorbate in units of gram per gram at equilibrium. Using the β value obtained from the graph, it is possible to evaluate the mean adsorption energy of the adsorption per mole of the adsorbate from the following equation:

$$E = \frac{1}{\sqrt{2\beta}} \quad (20)$$

The adsorption mean free energy is used to give information associated with the adsorption mechanism. If

the value of E calculated is below 8 kJ mol^{-1}, the adsorption is a physical process in nature and this value is between 8 and 16 kJ mol^{-1}, the adsorption type can be expressed by ion exchange, and over 16 kJ mol^{-1} it can be expressed by a stronger chemical adsorption than ion exchange [39,64,65].

Ammonium removal capacities of zeolite were tested with various adsorption isotherm models. For the efficient usage of zeolite as an adsorbent, it is essential to have chemicals models that help to define accurately NH_4-N equilibrium. Adsorption isotherm plots were drawn and the isotherm constants were detected using the linear equation of isotherm models Eqs. (10), (13), (15), and (18). A comparison of the adsorption isotherm constants and correlation coefficients obtained from different experimental conditions is showed in Table 5.

As is shown in Table 5, the isotherm models of Langmuir and Tempkin were accordant with the experimental data better than the other models ($R^2 > 0.95$). These models showed for the linear profile of the isotherm giving the highest value of R^2. The worst fits were found for the D–R isotherm model (0.61–0.95). Figs. 12, 13 and 14 show the Langmuir and Tempkin isotherm models plots for NH_4-N adsorption on natural zeolite.

When constants and correlation coefficients of D-R model examined, the correlation coefficients were observed to be lower 0.90 of R^2 in many cases. The graphs of the model in all experimental conditions are presented in supplementary Figs. S7(a), S8(a) and S9 (a). The value of E calculated was found lower than 8 kJ mol^{-1} in the maximum correlation coefficient of 0.9551, it means that the adsorption process is physical in nature. But, according to the data obtained from this model may not be accurate to comment on the adsorption mechanism.

As is seen from Table 5, the heterogeneity factor values of Freundlich isotherm model were $0 < 1/n < 1$ means that the adsorption process is favorable. However, these values of Freundlich isotherm were observed to be lower than the others in some cases ($R^2 < 0.95$) when the correlation coefficients were evaluated. The graphs of Freundlich isotherm model in all experimental conditions are presented in supplementary Figs. S7(b), S8(b) and S9(b). Although the Freundlich graph shows a linear curve, the curve seems to bend at higher values of C_e, as the adsorption gets close a maximum value, approving complete monolayer coverage of the adsorbent. From Table 5, Langmuir and Tempkin were more suitable according to the results obtained from the experimental data than the Freundlich isotherm due to the higher value of the correlations coefficient. Among the three parameter equations tested, the experimental results obtained from Langmuir and Tempkin isotherm models show the better and perfect fit.

The Langmuir model has several assumptions, such as constant adsorption energy and monolayer coverage. The graphs of Langmuir isotherm model in all cases are presented in Figs. 12(a), 13(a), and 14(a). The Langmuir monolayer capacity, q_m, values were found as 8.7719, 9.0744, and 9.1659 mg g^{-1} for 40°C, 200 rpm, −10 + 20 mesh to 0.9598, 0.9563, and 0.9956 of the maximum R^2 values, respectively. The separation factor R_L values were found between 0 and 1 indicate that the NH_4-N prefers to be in the bound state with surfaces and the nature of adsorption process is favorable. The adsorption of NH_4-N on natural zeolite follows the Langmuir isotherm model means that monolayer coverage occurs on the surface of the adsorbent. According to the results the monolayer formation during adsorption of NH_4-N is affirmed.

The graphs of Tempkin isotherm model in all cases are given in Figs. 12(b), 13(b), and 14(b). As shown in Table 5, in many cases the correlation coefficients of Tempkin isotherm model were observed to be higher than 0.95. The maximum R^2 values (>0.97) were found in the temperature of 25°C, the agitation speed of 200 rpm and the particle size of −20 + 35 mesh.

These parameters are similar the optimum experimental conditions found in the kinetic experiments. According to the results obtained from Tempkin isotherm model, it was observed to present better correlations than Freundlich and D–R model indicates that adsorption is detected by a uniform distribution of binding energies.

The maximum adsorption capacities of other adsorbent materials that were used for the ammonium adsorption from wastewaters are listed in Table 6. The Gördes zeolite in present study showed the highest performance among the other adsorbent materials. However, Gördes zeolite is more acceptable material as an adsorbent for adsorption of pollutants due to produce large quantities.

3.10. Regeneration and reuse of Gördes zeolite

Regeneration was applied to zeolite samples that were used for NH_4-N removal from landfill leachate. For this purpose, −10 + 20 mesh particle size of Gördes zeolite that had reached saturation with 1,384.4 mg L^{-1} NH_4-N containing landfill leachate was used in regeneration studies. Regeneration studies were conducted with 1/10 and 1/20 solid/liquid rate using 1-N NaCl and 2-N NaCl solutions at the temperature of 70°C and agitation speed of 200 rpm for contact time of 24 h. Then, they were washed with distilled water to

Table 5
Comparison of the adsorption isotherm constants obtained from different experimental conditions

	Freundlich constants			Langmuir constants				Tempkin constants				D–R constants			
	K_F	n	R^2	q_m	K_L	R_L	R^2	A	B	b	R^2	q_m	β	E	R^2
Temparature (°C)															
25	0.2302	1.662	0.8876	9.0744	0.00799	0.865–0.238	0.9563	0.0880	1.9662	1260.1572	0.9742	4.9620	110.0900	0.0674	0.8634
40	0.3876	1.898	0.8200	8.7719	0.0127	0.825–0.177	0.9598	0.1422	1.8666	1394.2133	0.9691	5.9512	76.8610	0.0807	0.9551
60	0.3621	1.863	0.9760	9.3023	0.0115	0.928–0.202	0.9535	0.1674	1.7517	1580.5951	0.9347	4.4053	12.3800	0.2010	0.7002
Agitation speed (rpm)															
100	0.2961	1.713	0.9482	11.0742	0.008236	0.939–0.219	0.9529	0.1240	2.0501	1208.5854	0.9353	4.5349	20.4350	0.1564	0.6299
200	0.2302	1.662	0.8876	9.0744	0.00799	0.865–0.238	0.9563	0.0880	1.9662	1260.1572	0.9742	4.9620	110.0900	0.0674	0.8634
300	1.0000	1.000	1.0000	10.5263	0.0113	0.940–0.186	0.9445	0.1988	1.8426	1344.6874	0.9119	96.2453	19.7520	0.1591	0.6087
Particle size (Mesh)															
−10 + 20	0.4764	1.96	0.9767	9.1659	0.0166	0.923–0.151	0.9956	0.2385	1.7308	1431.5467	0.9703	4.6711	8.5723	0.2415	0.7367
−20 + 35	0.2302	1.662	0.8876	9.0744	0.0079	0.865–0.238	0.9563	0.0880	1.9662	1260.1572	0.9742	4.9620	110.0900	0.0674	0.8634
−35 + 45	0.4592	1.913	0.9368	9.6805	0.0159	0.934–0.147	0.9867	0.2731	1.7128	1446.5910	0.9526	8.1866	3.6605	0.3696	0.8093
−45 + 65	0.4640	1.976	0.9358	8.8417	0.0171	0.905–0.125	0.9941	0.2284	1.7158	1444.0617	0.9735	4.8656	13.4930	0.1925	0.7894

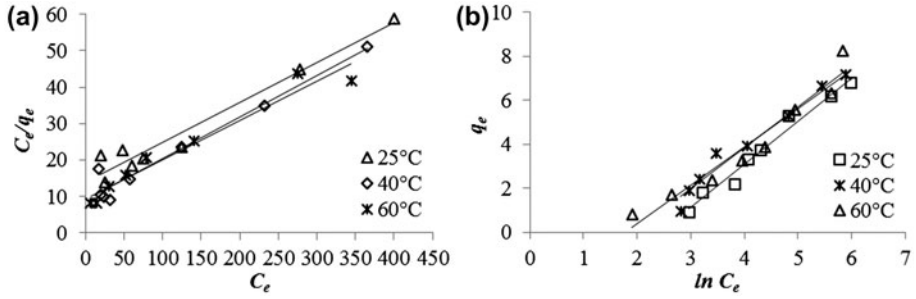

Fig. 12. Langmuir (a) and Tempkin (b) isotherm graphs at different temperature.

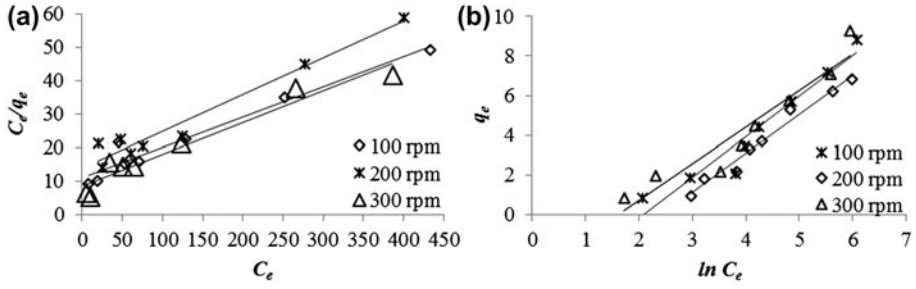

Fig. 13. Langmuir (a) and Tempkin (b) isotherm graphs for different agitation speed.

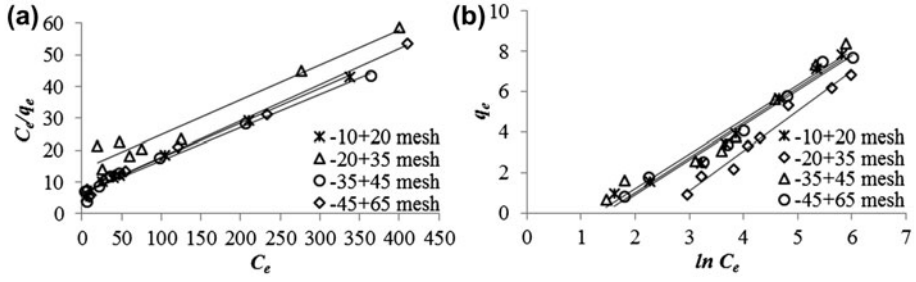

Fig. 14. Langmuir (a) and Tempkin (b) isotherm graphs for different particle size.

clean Cl^- ions and dried at 35–60°C for the moisture. Reuse of zeolite samples regenerated was examined at the temperature of 25 ± 3°C with contact time of 1 h, agitation speed of 200 rpm, its pH value of leachate, and initial concentration of 1,204 mg L^{-1}.

The results obtained from reuse of zeolite regenerated are given in Fig. 15. As it is seen from Fig. 15, it was observed that the removal efficiencies were decreased a rate of 25% in conducted studies for reuse of zeolite sample regenerated to remove NH_4-N from landfill leachate.

While removal efficiency of natural zeolite was around 49%, NH_4-N removal performances of preconditioning zeolite with 1-N and 2-N NaCl were 78 and 81%, respectively. Waste zeolite samples regenerated with 1/10 solid/liquid rate using 1-N NaCl and 2-N NaCl solutions after these experiments were reused and NH_4-N removal performances of these zeolite samples were found 50 and 62%, respectively. The differences of removal efficiencies were clearly seen from figure. Therefore, the implementation of the regeneration process means extra cost and lower efficiency. However, application of regeneration process is transformed into a disadvantage when considering treatment of concentrated wastewater.

3.11. Thermodynamic analysis

The thermodynamic activation parameters such as the Gibbs free energy change of adsorption (ΔG°), the

Table 6
Comparison of the adsorption capacities of Gördes zeolite with those of other adsorbent materials

Adsorbents	Maximum adsorption capacity (mg g^{-1})	Refs.
Boston ivy leaf powder (BPTL)	6.59	[66]
Sepiolite	1.47	[67]
Sawdust	1.70	[68]
Chabazite	2.94	[69]
Activated sludge	0.40	[70]
P. oceanica fibers	1.73	[71]
Natural zeolite	1.00	[72]
Zeolite	8.91	[73]
Zeolite	7.50	[74]
Zeolite	4.49	[37]
Zeolite	8.71	[75]
Zeolite 13X	8.61	[76]
Natural Chinese clinoptilolite	2.02	[77]
Clinoptilolite	6.32	[78]
Clinoptilolite	5.74	[79]
Silicate-carbon modified zeolite	0.12	[80]
NaOH-activated zeolite	4.55	[81]
NaCl-activated zeolite	5.92	[81]
Zeolite synthesized from fly ash	0.90	[82]
Activated zeolite with NaCl	9.07	Present study

entropy change (ΔH°), and the enthalpy change (ΔS°) are determined using following equations. These parameters are obtained from the variation of Langmuir constant (K_c) changing with temperature as follows [8,61,81,83]:

$$K_c = \frac{q_e}{C_e} \tag{21}$$

$$\Delta G^\circ = -RT \ln K_c \tag{22}$$

$$\Delta G^\circ = \Delta H^\circ - T\Delta S^\circ \tag{23}$$

$$\ln K_c = -\frac{\Delta H^\circ}{RT} + \frac{\Delta S^\circ}{R} \tag{24}$$

where K_c is the equilibrium constant, which can be obtain from Langmuir isotherms at different temperature (mL g^{-1}), K_c is calculated by multiplying the constants calculated from the Langmuir isotherm model. C_e is the equilibrium concentration in solution (mg L^{-1}) and q_e is the amount of adsorbate adsorbed at equilibrium (mg g^{-1}), R is the universal gas constant (8.314 J K^{-1} mol^{-1}), T is absolute temperature (K), ΔH° is the standard enthalpy change (kJ mol^{-1}), ΔS° is the standard entropy change (J mol^{-1} K^{-1}), and ΔG° is the Gibbs free energy (kJ mol^{-1}).

When $\ln K_c$ is plotted vs. $1/T$, a linear plot namely Van't Hoff plot yields $\Delta H^\circ/R$ as the slope and $\Delta S^\circ/R$ as the intercept from which values of ΔH° and ΔS° are obtained (Fig. 16).

The influence of temperature on NH_4-N removal was performed at 25, 40, and 60°C. Thermodynamic parameters obtained from the graph are listed in Table 7. The Gibbs free energy change of adsorption gives information about the degree of spontaneity of the adsorption process [84]. The ΔG° values obtained from the thermodynamic calculations change from 5.7113 to 6.5018 kJ mol^{-1} for NH_4-N. According to the positive ΔG° values, the adsorption process was not spontaneous thermodynamically.

The standard entropy is used to describe whether the reaction is identified with associative or dissociative mechanism [65,83]. The standard entropy changes, ΔS°, for the adsorption process was calculated as

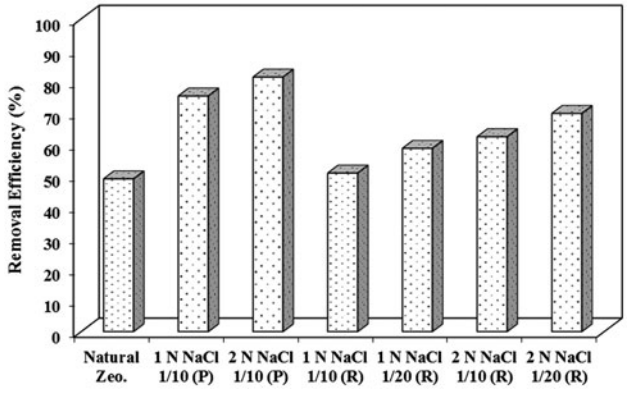

Fig. 15. Reuse of zeolite after preconditioning (P) and regeneration (R).

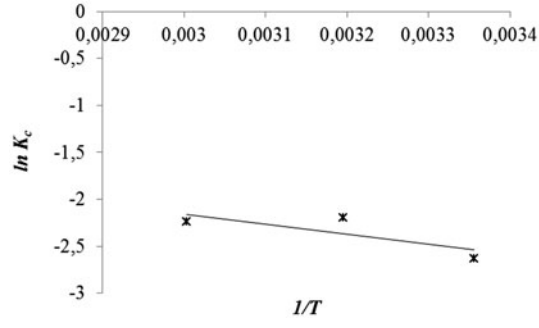

Fig. 16. Van't Hoff plot for the adsorption of NH_4-N in landfill leachate by zeolite.

Table 7
Thermodynamic parameters for the adsorption of NH_4-N by zeolite

Temperature (K)	K_c	ΔG° (kJ mol^{-1})	ΔH° (kJ mol^{-1})	ΔS° (J mol^{-1} K^{-1})	R^2
298	0.0725	6.5018	−8.5415	8.8209	0.6241
313	0.1114	5.7113			
333	0.1070	6.1885			

8.8209 J mol^{-1} K^{-1}. The positive value of ΔS° reflects the affinity of zeolite for NH_4-N. The positive value of ΔS° shows that there is an increase in the randomness in the adsorbent/adsorbate interface during the adsorption process.

The standard enthalpy change, ΔH°, also provides information us about the type of adsorption whether the adsorption is physical or chemical process [85]. The enthalpy change of the adsorption process was calculated as a negative value of −8.5415 kJ mol^{-1} from the Van't Hoff plot. This value showed to be the exothermic nature of the adsorption process. Also, the adsorption process was controlled by physical mechanism rather than chemical mechanism. Therefore, NH_4-N adsorption was an exothermic process and physical mechanism.

4. Conclusions

In present study, the removal of NH_4-N from landfill leachate by batch adsorption technique was researched. The results obtained from this study are presented below as articles:

(1) Adsorption process is a powerful alternative among the other NH_4-N removal technologies due to ease of operation.
(2) Gördes zeolite is an influential and a low-cost alternative adsorbent for the removal of NH_4-N from landfill leachate.
(3) The Gördes zeolite showed the highest performance with the maximum adsorption capacity of 9.07 mg g^{-1} compared to the other adsorbent materials.
(4) The pseudo-second-order reaction kinetic model was determined to be the best correlation according to the results obtained from the kinetic experiments for NH_4-N removal from landfill leachate using zeolite. Thus, it shows that the rate limiting step can be chemisorption rather than diffusion.
(5) The results obtained from the equilibrium studies show that the best fitted adsorption isotherm models were detected as follows: Langmuir–Tempkin > Freundlich > Dubinin–Raduhkevich.
(6) Thermodynamic parameters are showed that the adsorption of NH_4-N on zeolite was not spontaneous, was an exothermic process and physical mechanism, and showed the increasing randomness. The thermodynamic parameters suggest that the adsorption process can be applied for the NH_4-N removal by zeolite.

According to the all results, it is finalized that Gördes zeolite has a good adsorption performance and can be successfully used for NH_4-N removal from landfill leachate.

Supplementary material

The supplementary material for this paper is available online at http://dx.doi.10.1080/19443994.2015.1136964.

Acknowledgments

This work was financed by a scholarship of the Ondokuz Mayıs University for support of Scientific/Technological Research (Project MF-054). I thank the Ondokuz Mayıs University for providing the opportunity to research.

References

[1] D.H. Ahn, Y.C. Chung, W.S. Chang, Use of coagulant and zeolite to enhance the biological treatment efficiency of high ammonia leachate, J. Environ. Sci. Health Part A 37(2) (2002) 163–173.
[2] M.R. Boni, A. Chiavola, S. Sbaffoni, Pretreated waste landfilling: Relation between leachate characteristics and mechanical behaviour, Waste Manage. 26 (2006) 1156–1165.
[3] J. Rodríguez, L. Castrillón, E. Marañón, H. Sastre, E. Fernández, Removal of non-biodegradable organic matter from landfill leachates by adsorption, Water Res. 38 (2004) 3297–3303.
[4] C.D. Iaconi, R. Ramadori, A. Lopez, Combined biological and chemical degradation for treating a mature municipal landfill leachate, Biochem. Eng. J. 31 (2006) 118–124.
[5] R. He, X.W. Liu, Z.J. Zhang, D.S. Shen, Characteristics of the bioreactor landfill system using an anaerobic–aerobic process for nitrogen removal, Bioresour. Technol. 98 (2007) 2526–2532.

[6] Y. Wang, S. Lıu, Z. Xu, T. Han, S. Chuan, T. Zhu, Ammonia removal from leachate solution using natural Chinese clinoptilolite, J. Hazard. Mater. 136 (2006) 735–740.
[7] A. Kuleyin, Removal of phenol and 4-chlorophenol by surfactant-modified natural zeolite, J. Hazard. Mater. 144 (2007) 307–315.
[8] N.G. Turan, Metal uptake from aqueous leachate of poultry litter by natural zeolite, Environ. Progress Sustainable Energy 30 (2010) 152–159.
[9] N.G. Turan, O.N. Ergun, Removal of Cu(II) from leachate using natural zeolite as a landfill liner material, J. Hazard. Mater. 167 (2009) 696–700.
[10] N.G. Turan, B. Mesci, O. Ozgonenel, The use of artificial neural networks (ANN) for modeling of adsorption of Cu(II) from industrial leachate by pumice, Chem. Eng. J. 171 (2011) 1091–1097.
[11] N.G. Turan, S. Elevli, B. Mesci, Adsorption of copper and zinc ions on illite: Determination of the optimal conditions by the statistical design of experiments, Appl. Clay Sci. 52 (2011) 392–399.
[12] N.G. Turan, B. Mesci, O. Ozgonenel, Artificial neural network (ANN) approach for modeling Zn(II) adsorption from leachate using a new biosorbent, Chem. Eng. J. 173 (2011) 98–105.
[13] N.G. Turan, O. Ozgonenel, Optimizing copper ions removal from industrial leachate by explored vermiculite—A comparative analysis, J. Taiwan Inst. Chem. Eng. 44 (2013) 895–903.
[14] M. Malandrino, O. Abollino, A. Giacomino, M. Aceto, E. Mentasti, Adsorption of heavy metals on vermiculite: Influence of pH and organic ligands, J. Colloid Interface Sci. 299 (2006) 537–546.
[15] N.G. Turan, O. Özgonenel, Study of montmorillonite clay for the removal of copper (II) by adsorption: Full factorial design approach and Cascade Forward Neural Network, Sci. World J. 2013 (2013) 1–12, doi: 10.1155/2013/342628.
[16] T. Boonfueng, L. Axe, Y. Xu, T.A. Tyson, Nickel and lead sequestration in manganese oxide-coated montmorillonite, J. Colloid Interface Sci. 303 (2006) 87–98.
[17] M. Karatas, Removal of Pb(II) from water by natural zeolitic tuff: Kinetics and thermodynamics, J. Hazard. Mater. 199–200 (2012) 383–389.
[18] T.K. Naiya, A.K. Bhattacharya, S.K. Das, Clarified sludge (basic oxygen furnace sludge)—An adsorbent for removal of Pb(II) from aqueous solutions—Kinetics, thermodynamics and desorption studies, J. Hazard. Mater. 170 (2009) 252–262.
[19] K.S. Low, C.K. Lee, A.C. Leo, Removal of metals from electroplating wastes using banana pith, Bioresour. Technol. 51 (1995) 227–231.
[20] S.C. Pan, C.C. Lin, D.H. Tseng, Reusing sewage sludge ash as adsorbent for copper removal from wastewater, Resour. Conserv. Recycl. 39 (2003) 79–90.
[21] A.R. Wilson, L.W. Lion, Y.M. Nelson, Pb scavenging from a freshwater lake by Mn oxides in heterogeneous surface coating materials, Environ. Sci. Technol. 35 (2001) 3182–3189.
[22] M. Ajmal, A.H. Khan, S. Ahmad, A. Ahmad, Role of sawdust in the removal of copper(II) from industrial wastes, Water Res. 32 (1998) 3085–3091.
[23] M.E. Argun, S. Dursun, C. Ozdemir, M. Karatas, Heavy metal adsorption by modified oak sawdust: Thermodynamics and kinetics, J. Hazard. Mater. 141 (2007) 77–85.
[24] B.M.W.P.K. Amarasinghe, R.A. Williams, Tea waste as a low cost adsorbent for the removal of Cu and Pb from wastewater, Chem. Eng. J. 132 (2007) 299–309.
[25] A. Shafaei, F.Z. Ashtiani, T. Kaghazchi, Equilibrium studies of the sorption of Hg(II) ions onto chitosan, Chem. Eng. J. 133 (2007) 311–316.
[26] N. Li, R. Bai, Copper adsorption on chitosan–cellulose hydrogel beads: Behaviors and mechanisms, Sep. Purif. Technol. 42 (2005) 237–247.
[27] G.E. Márquez, M.J.P. Ribeiro, J.M. Ventura, J.A. Labrincha, Removal of nickel from aqueous solutions by clay-based beds, Ceram. Int. 30 (2004) 111–119.
[28] S.M. Auerbach, K.A. Carrado, P.K. Dutta, Handbook of Zeolite Science and Technology, Basel, New York, NY, 2003.
[29] O. Ozdemir, B. Armagan, M. Turan, M.S. Çelik, Comparison of the adsorption characteristics of azo-reactive dyes on mezoporous minerals, Dyes Pigm. 62 (2004) 49–60.
[30] Ö. Çağlar Duvarcı, Y. Akdeniz, F. Özmıhçı, S. Ülkü, D. Balköse, M. Çiftçioğlu, Thermal behaviour of a zeolitic tuff, Ceram. Int. 33(5) (2007) 795-801.
[31] A.E. Osmanlioglu, Treatment of radioactive liquid waste by sorption on natural zeolite in Turkey, J. Hazard. Mater. 137 (2006) 332–335.
[32] D. Karadag, S. Tok, E. Akgul, M. Turan, M. Ozturk, A. Demir, Ammonium removal from sanitary landfill leachate using natural Gördes clinoptilolite, J. Hazard. Mater. 153 (2008) 60–66.
[33] M. Kithome, J.W. Paul, L.M. Lavkulich, A.A. Bomke, Kinetics of ammonium adsorption and desorption by the natural zeolite clinoptilolite, Soil Sci. Soc. Am. J. 62 (1998) 622–629.
[34] APHA, AWWA, WEF, Standard Methods for the Examination of Water and Wastewater, American Public Health Association, Washington, DC, eighteenth ed., 1985.
[35] I.D. Mall, V.C. Srivastava, N.K. Agarwal, Removal of Orange-G and Methyl Violet dyes by adsorption onto bagasse fly ash—Kinetic study and equilibrium isotherm analyses, Dyes Pigm. 69 (2006) 210–223.
[36] N. Bektaş, S. Kara, Removal of lead from aqueous solutions by natural clinoptilolite: Equilibrium and kinetic studies, Sep. Purif. Technol. 39 (2004) 189–200.
[37] D. Karadag, Y. Koc, M. Turan, M. Ozturk, A comparative study of linear and non-linear regression analysis for ammonium exchange by clinoptilolite zeolite, J. Hazard. Mater. 144 (2007) 432–437.
[38] N.P. Hankins, S. Pliankarom, N. Hilal, An equilibrium ion exchange study on the removal of NH_4 ion from aqueous effluent using clinoptilolite, Sep. Sci. Technol. 39(15) (2004) 3639.
[39] N. Azouaou, Z. Sadaoui, A. Djaafri, H. Mokaddem, Adsorption of cadmium from aqueous solution onto untreated coffee grounds: Equilibrium, kinetics and thermodynamics, J. Hazard. Mater. 184 (2010) 126–134.
[40] S. Malamis, E. Katsou, A review on zinc and nickel adsorption on natural and modified zeolite, bentonite and vermiculite: Examination of process parameters, kinetics and isotherms, J. Hazard. Mater. 252–253 (2013) 428–461.

[41] K. Vijayaraghavan, Y.S. Yun, Bacterial biosorbents and biosorption, Biotechnol. Adv. 26 (2008) 266–291.
[42] D. Park, Y.S. Yun, J.M. Park, The past, present, and future trends of biosorption, Biotechnol. Bioprocess Eng. 15 (2010) 86–102.
[43] Y.S. Ho, Review of second-order models for adsorption systems, J. Hazard. Mater. 136 (2006) 681–689.
[44] N. Bektaş, B.A. Ağım, S. Kara, Kinetic and equilibrium studies in removing lead ions from aqueous solutions by natural sepiolite, J. Hazard. Mater. 112 (2004) 115–122.
[45] W.J. Weber, J.C. Morris, Kinetics of adsorption on carbon solution, J. Sanit. Eng. Div. Am. Soc. Civ. Eng. 89 (1963) 31–60.
[46] P.S. Kumar, S. Ramalingam, S.D. Kirupha, A. Murugesan, T. Vidhyadevi, S. Sivanesan, Adsorption behavior of nickel(II) onto cashew nut shell: Equilibrium, thermodynamics, kinetics, mechanism and process design, Chem. Eng. J. 167 (2011) 122–131.
[47] Y. Önal, Kinetics of adsorption dyes from aqueous solution using activated carbon prepared from waste apricot, J. Hazard. Mater. B137 (2006) 1719–1728.
[48] D. Wen, Y.S. Ho, X. Tang, Comparative sorption kinetic studies of ammonium onto zeolite, J. Hazard. Mater. 133 (2006) 252–256.
[49] P. Liao, S. Yuan, W. Zhang, M. Tong, K. Wang, Mechanistic aspects of nitrogen heterocyclic compound adsorption on bamboo charcoal, J. Colloid Interface Sci. 382 (2012) 74–81.
[50] S. Lagergren, Zur theorie der sogenannten adsorption geloster stoffe, Kungliga Sevenska Vetenskapasakademiens, Handlingar 24(7) (1898) 1–3.
[51] Y.S. Ho, G. McKay, Pseudo-second order model for sorption processes, Process Biochem. 34 (1999) 451–465.
[52] Y. Chen, D. Zhang, Adsorption kinetics, isotherm and thermodynamics studies of flavones from Vaccinium Bracteatum Thunb leaves on NKA-2 resin, Chem. Eng. J. 254 (2014) 579–585.
[53] M. Kapur, M.K. Mondal, Competitive sorption of Cu (II) and Ni(II) ions from aqueous solutions: Kinetics, thermodynamics and desorption studies, J. Taiwan Inst. Chem. Eng. 45 (2014) 1803–1813.
[54] I. Langmuir, The adsorption of gases on plane surfaces of glass, mica and platinum, J. Am. Chem. Soc. 40 (1918) 1361–1403.
[55] A. Olgun, N. Atar, Equilibrium, thermodynamic and kinetic studies for the adsorption of lead (II) and nickel (II) onto clay mixture containing boron impurity, J. Ind. Eng. Chem. 18 (2012) 1751–1757.
[56] H.M.F. Freundlich, Uber die adsorption in losungen, Zeitschrift fur physikalische chemie (Leipzig), 57A (1906) 385–470.
[57] A. Kuleyin, F. Aydin, Removal of reactive textile dyes (Remazol Brillant Blue R and Remazol Yellow) by surfactant-modified natural zeolite, Environ. Progress Sustainable Energy 30 (2011) 141–151.
[58] K.K.H. Choy, G. McKay, J.F. Porter, Sorption of acid dyes from effluents using activated carbon, Resour. Conserv. Recycl. 27 (1999) 57.
[59] C.T. Hsieh, H. Teng, Liquid phase adsorption of phenol onto activated carbon prepared with different activation levels, J. Colloid Interface Sci. 230 (2000) 171–175.
[60] S. Madala, S.K. Nadavala, S. Vudagandla, V.M. Boddu, K. Abburi, Equilibrium, kinetics and thermodynamics of Cadmium (II) biosorption on to composite chitosan biosorbent, Arab. J. Chem. (2013), doi: 10.1016/j.arabjc.2013.07.017.
[61] K.G. Akpomie, F.A. Dawodua, Efficient abstraction of nickel(II) and manganese(II) ions fromsolution onto an alkaline-modified montmorillonite, J. Taibah Univ. Sci. 8 (2014) 343–356, doi: 10.1016/j.jtusci.2014.05.001.
[62] T. Salman, F. Aydın Temel, G. Turan, Y. Ardalı, Removal of lead (II) from aqueous solution by batch adsorption on various inexpensive adsorbents using experimental design, Desalin. Water Treat. 56 (2014) 1566–1575, doi: 10.1080/19443994.2014.951073.
[63] M.M. Dubinin, L.V. Radushkevich, Equation of the characteristic curve of activated charcoal, Proc. Acad. Sci. USSR 55 (1947) 331–333.
[64] B. Singha, S.K. Das, Biosorption of Cr(VI) ions from aqueous solutions: Kinetics, equilibrium, thermodynamics and desorption studies, Colloids Surf., B: Biointerfaces 84 (2011) 221–232.
[65] I. Mobasherpour, E. Salahi, M. Ebrahimi, Thermodynamics and kinetics of adsorption of Cu(II) from aqueous solutions onto multi-walled carbon nanotubes, J. Saudi Chem. Soc. 18 (2011) 792–801, doi: 10.1016/j.jscs.2011.09.006.
[66] H. Liu, Y. Dong, H. Wang, Y. Liu, Adsorption behavior of ammonium by a bioadsorbent—Boston ivy leaf powder, J. Environ. Sci. 22(10) (2010) 1513–1518.
[67] M.P. Bernal, J.M. Lopez-Real, Natural zeolites and sepiolite as ammonium and ammonia adsorbent materials, Bioresour. Technol. 43 (1993) 27–33.
[68] M.A. Wahab, S. Jellali, N. Jedidi, Ammonium biosorption onto sawdust: FTIR analysis, kinetics and adsorption isotherms modeling, Bioresour. Technol. 101 (2010) 5070–5075.
[69] O. Lahav, M. Green, Ammonium removal using ion exchange and biological regeneration, Water Res. 32(7) (1998) 2019–2028.
[70] P.H. Nielsen, Adsorption of ammonium to activated sludge, Water Res. 30 (1996) 762–764.
[71] S. Jellali, M.A. Wahab, M. Anane, K. Riahi, N. Jedidi, Biosorption characteristics of ammonium from aqueous solutions onto *Posidonia oceanica* (L.) fibers, Desalination 270 (2011) 40–49.
[72] M. Sarioglu, Removal of ammonium from municipal wastewater using natural Turkish (Dogantepe) zeolite, Sep. Purif. Technol. 41 (2005) 1–11.
[73] M. Lebedynets, M. Sprynskyy, I. Sakhnyuk, R. Zbytniewski, R. Golembiewski, B. Buszewski, Adsorption of ammonium ıons onto a natural zeolite: Transcarpathian clinoptilolite, Adsorpt. Sci. Technol. 22 (2004) 731–741.
[74] K. Saltalı, A. Sarı, M. Aydın, Removal of ammonium ion from aqueous solution by natural Turkish (Yıldızeli) zeolite for environmental quality, J. Hazard. Mater. 141 (2007) 258–263.
[75] Y. Wang, F. Lin, W. Pang, Ammonium exchange in aqueous solution using Chinese natural clinoptilolite and modified zeolite, J. Hazard. Mater. 142 (2007) 160–164.
[76] H. Zheng, L. Han, H. Ma, Y. Zheng, H. Zhang, D. Liu, S. Liang, Adsorption characteristics of ammonium ion by zeolite 13X, J. Hazard. Mater. 158 (2008) 577–584.

[77] Y. Wang, S. Lıu, Z. Xu, T. Han, S. Chuan, T. Zhu, Ammonia removal from leachate solution using natural Chinese clinoptilolite, J. Hazard. Mater. 136 (2006) 735–740.
[78] D. Karadag, Y. Koc, M. Turan, B. Armagan, Removal of ammonium ion from aqueous solution using natural Turkish clinoptilolite, J. Hazard. Mater. 136 (2006) 604–609.
[79] M.L. Nguyen, C.C. Tanner, Ammonium removal from wastewaters using natural New Zealand zeolites, New Zealand J. Agric. Res. 41 (1998) 427–446.
[80] M. Li, X. Zhu, F. Zhu, G. Ren, G. Cao, L. Song, Application of modified zeolite for ammonium removal from drinking water, Desalination 271 (2011) 295–300.
[81] A. Alshameri, C. Yan, Y. Al-Ani, A.S. Dawood, A. Ibrahim, C. Zhou, H. Wang, An investigation into the adsorption removal of ammonium by salt activated Chinese (Hulaodu) natural zeolite: Kinetics, isotherms, and thermodynamics, J. Taiwan Inst. Chem. Eng. 45 (2014) 554–564.
[82] D. Wu, B. Zhang, C. Li, Z. Zhang, H. Kong, Simultaneous removal of ammonium and phosphate by zeolite synthesized from fly ash as influenced by salt treatment, J. Colloid Interface Sci. 304 (2006) 300–306.
[83] X. Zhao, G. Zhang, Q. Jia, C. Zhao, W. Zhou, W. Li, Adsorption of Cu(II), Pb(II), Co(II), Ni(II), and Cd(II) from aqueous solution by poly(aryl ether ketone) containing pendant carboxyl groups (PEK-L): Equilibrium, kinetics, and thermodynamics, Chem. Eng. J. 171 (2011) 152–158.
[84] N. Boujelben, J. Bouzid, Z. Elouear, Adsorption of nickel and copper onto natural iron oxide-coated sand from aqueous solutions: Study in single and binary systems, J. Hazard. Mater. 163 (2009) 376–382.
[85] M.E. Argun, Use of clinoptilolite for the removal of nickel ions from water: Kinetics and thermodynamics, J. Hazard. Mater. 150 (2008) 587–595.